



## Original article

## *Plumbago zeylanica* L. exhibited potent anticancer activity in Ehrlich ascites carcinoma bearing Swiss albino mice

Neha Sharma<sup>a</sup>, Shubham Thakur<sup>b</sup>, Rasdeep Kour<sup>a</sup>, Deepika<sup>c</sup>, Ajay Kumar<sup>d</sup>, Ajaz Ahmad<sup>e</sup>, Prashant Kaushik<sup>f</sup>, Vaseem Raja<sup>d,\*</sup>, Subheet Kumar Jain<sup>b</sup>, Satwinderjeet Kaur<sup>a,\*</sup>

<sup>a</sup> Department of Botanical and Environmental Sciences, Guru Nanak Dev University, Amritsar 143005, Punjab, India

<sup>b</sup> Department of Pharmaceutical Sciences, Guru Nanak Dev University Amritsar 143005, Punjab, India

<sup>c</sup> Department of Geography, Baba Mastnath University (BMU), Asthal Bohar, Rohtak 124001, Haryana, India

<sup>d</sup> University Center for Research & Development (UCRD), Biotechnology Engineering & Food Technology, Chandigarh University, Gharuan, Mohali 140413, Punjab, India

<sup>e</sup> Department of Clinical Pharmacy, College of Pharmacy, King Saud University, Riyadh 11451, Saudi Arabia

<sup>f</sup> Instituto de Conservación y Mejora de la Agrodiversidad Valenciana, Universitat Politècnica de València, 46022 Valencia, Spain



## ARTICLE INFO

## Article history:

Received 29 July 2023

Revised 2 October 2023

Accepted 4 October 2023

Available online 7 October 2023

## Keywords:

Anticancer

Apoptosis

EAC

Cell Cycle

*Plumbago zeylanica*

## ABSTRACT

**Objectives:** We investigated the anticancer activity of the PzMH fraction (hexane fraction) extracted from the roots of *Plumbago zeylanica* L., an ethnomedicinally significant plant widely distributed in India.

**Methods:** The PzMH fraction was obtained through rigorous extraction and purification processes. In vitro cytotoxicity assays were performed to assess its effects on Ehrlich ascites carcinoma (EAC) cells. Acute toxicity studies were conducted to evaluate its safety profile. An *in vivo* study was carried out on EAC-bearing Swiss albino mice to assess its anticancer efficacy. Flow cytometric and microscopic analyses were done to examine the induction of cell death by the PzMH fraction. Western blot analysis was used to investigate the molecular mechanisms involved.

**Results:** The PzMH fraction exhibited a significant cytotoxic effect *in vitro*, resulting in 50% cell death in EAC cells at low concentrations. The calculated GI<sub>50</sub> value for the PzMH fraction was 42.74 µg/ml, demonstrating a comparable efficacy to the standard drug 5-fluoro uracil (GI<sub>50</sub> = 43.38 µg/ml). The safety of therapeutic doses was confirmed through acute toxicity studies, which yielded an LD<sub>50</sub> value of 500 mg/kg body weight. In the *in vivo* study, the PzMH fraction demonstrated a substantial 79.05% inhibition in the growth of EAC cells at the 300 mg/kg body weight dose of PzMH fraction. Flow cytometric and microscopic analyses revealed distinct apoptotic features in EAC cells treated with the PzMH fraction. Cell cycle analysis showed a significant arrest at the G<sub>0</sub>/G<sub>1</sub> stage following treatment. PzMH treatment elicited a response characterized by escalated levels of cleaved caspases-3 and -9, while concurrently leading to a decreased expression of the Bcl2 protein, as evidenced by Western blot analysis.

**Conclusions:** The current research provides empirical evidence supporting the anticancer activity of the PzMH fraction extracted from *P. zeylanica*. The observed cytotoxicity, safety, and apoptosis-inducing properties make it a promising candidate for further investigation as a potential cancer therapy. Further exploration of its phytochemical composition, including major compounds such as 4-hydroxybenzaldehyde, *trans*-cinnamic acid, plumbagin and lawsone, contributes to our understanding of its mechanisms of action.

© 2023 The Authors. Published by Elsevier B.V. on behalf of King Saud University. This is an open access article under the CC BY license (<http://creativecommons.org/licenses/by/4.0/>).

\* Corresponding authors.

E-mail addresses: [wrajamp2009@gmail.com](mailto:wrajamp2009@gmail.com) (V. Raja), [satwinderjeet.botenv@ndu.ac.in](mailto:satwinderjeet.botenv@ndu.ac.in) (S. Kaur).

Peer review under responsibility of King Saud University.



Production and hosting by Elsevier

### 1. Introduction

Cancer poses a formidable worldwide health crisis, accounting for approximately 10 million annual fatalities. Cancer is a multi-stage disease characterized by a lack of programmed cell death and uncontrolled cell division leading to invasion in neighbouring tissues (Alvarez-Ortega et al., 2023). In India, 1.46 million cases of cancer were estimated in 2022 and it is predicted to rise up to 1.57 million by 2025 (Sathishkumar et al., 2022). The biological

<https://doi.org/10.1016/j.jksus.2023.102932>

1018-3647/© 2023 The Authors. Published by Elsevier B.V. on behalf of King Saud University.

This is an open access article under the CC BY license (<http://creativecommons.org/licenses/by/4.0/>).

functions of normal cells in the body are controlled by various intricate and interconnected signaling pathways which are mostly dysregulated in the cancer cells (Hashem et al., 2022). Cancer is characterized by distinct features, including uncontrolled cell growth, the formation of new blood vessels (angiogenesis), the ability to spread to distant sites (metastasis), invasion into nearby tissues, disrupted metabolic processes, and evasion of programmed cell death and growth-inhibiting signals (Hanahan, 2022). The importance of apoptosis in cancer has drawn a lot of attention, and it is now commonly acknowledged that cancer cells can acquire the ability to fight apoptosis, giving them a survival advantage that encourages tumor development and treatment failure (Morana et al., 2022). Therefore, targeting the proteins involved in inhibiting and initiating apoptotic pathways is critical to developing effective therapeutics against cancer. Despite the substantial research carried out over the previous decades, there are still no effective therapeutic options for cancer. Existing clinical remedies, such as chemotherapy and radiotherapy, face limitations in acceptability and clinical applicability due to their systemic toxicity. (Kashyap et al., 2021). Over the past few decades, extensive research has shown that natural compounds isolated from the medicinal plants are a better substitute to prevent and cure cancer as these are low-cost and have minimal side effects on normal cells (Safarzadeh et al., 2014). The history of the development of anticancer drugs has been shaped by natural products. Many commonly used anticancer medications come from plants, including irinotecan, vincristine, etoposide, and paclitaxel (Huang et al., 2021).

*Plumbago zeylanica* L., a highly potent medicinal herb found abundantly across India, is a key ingredient in numerous Ayurvedic formulations. In traditional medicine practices, it is employed to treat a range of conditions, including chronic coughs and colds, enlarged spleen and liver, neural disorders, and microbial infections (Shukla et al., 2021). It contains a variety of bioactive substances with documented antioxidant, anti-obesity, anti-diabetic, anti-microbial, anti-malarial, and wound-healing activities (Bloch et al., 2022). The aforementioned bioactivities prompted us to investigate this plant's anticancer potential in mice bearing Ehrlich Ascites Carcinoma (EAC). EAC, often described as an undifferentiated carcinoma, is primarily hyperdiploid, highly transplantable, never regresses, proliferates quickly, has a reduced life expectancy, and lacks tumor-specific transplantation antigens. It is the most used experimental tumor model because it closely resembles human tumors and is highly transplantable, making it easy to transplant from one animal to another (Ozaslan et al., 2011).

### 1.1. Procurement and authentication of plant material

*Plumbago zeylanica* L. roots were purchased from Majith Mandi, Amritsar, authenticated by Dr. Narendra Kumar (Scientist) at CSIR-CIMAP, Lucknow and deposited in the crude drug repository at CSIR-CIMAP with an accession number P035.

### 1.2. PzMH fraction extraction

To obtain the PzMH fraction from the plant material, a systematic process was followed. The plant material (1 kg) grinded into powdered form and macerated into cold hexane with regular agitation. Following maceration, the mixture was filtered to separate the liquid hexane extract from any solid residues. The concentrated PzMH fraction was obtained by removing the hexane solvent from the extract under reduced pressure using a rotavapor.

### 1.3. Animal Ethics statement

The *in-vivo* experiments were performed on 10–16 weeks old Swiss albino female mice. The present study adhered to approved animal experimentation protocols. The IAEC at GNDU, Amritsar, granted approval in accordance with CPCSEA regulations (226/CPCSEA/2019/25). All animal experiments strictly followed the guidelines for animal experimentation set forth by CPCSEA, Government of India, New Delhi.

### 1.4. Procurement and care of animals under experimentation

The Swiss albino mice used in the study were sourced from the NIPER, Mohali, Punjab. Animals were acclimatized and housed in well-maintained cages at GNDU, Amritsar, Punjab. They were fed commercial rodent feed and water.

### 1.5. Acute toxicity studies

The acute toxicity of the PzMH fraction was examined in female Swiss albino mice according to OECD guidelines 423 (Organisation for Economic Co-operation and Development, 2017) (Toxicity-Up, 2001); [OECD Test Guideline 423 (nih.gov)].

## 2. Evaluation of *in-vivo* anticancer potential using EAC (Ehrlich ascites Carcinoma) model

### 2.1. Procurement and maintenance of cell lines

The EAC cells were collected from NCCS, Pune, India. Subsequently, cells were procured under controlled conditions, precisely maintained within a CO<sub>2</sub> incubator at 37 °C. The culture medium used for their propagation was the Minimum Essential Medium, supplemented with 10% heat-inactivated Fetal Bovine Serum (FBS) and ensuring optimal growth and maintenance.

### 2.2. *In vitro* cytotoxicity analysis using MTT assay

The MTT assay was used to quantify the *in vitro* cytotoxicity of PzMH fraction on EAC cells. In 96-well plates, EAC cells (passage number-32) were cultured and subjected to various concentrations of the PzMH fraction and 5-fluorouracil (50, 100, 200, 400, 800 µg/ml) for a duration of 24 h. After the incubation period, each well received 0.02 ml of MTT solution (5 mg/ml) and was subsequently incubated for 5 h at 37 °C in a CO<sub>2</sub> incubator. Media was removed from each well following incubation with MTT and 100 µl DMSO was added in each well and absorbance was recorded at 570 nm using multimode multiplate reader (BioTek Synergy HT, Winooski, USA) (Islam et al., 2015). The subsequent equation served as the basis for computing the growth inhibition.

$$\% \text{Growth inhibition} = \frac{A_C - A_T}{A_C} \times 100$$

A<sub>C</sub>: Absorbance of control (untreated) cells

A<sub>T</sub>: Absorbance of treated cells

### 2.3. *In-vivo* experimental design

Swiss albino mice weighing between 18 and 25 g were allocated into five groups, each comprising six animals. Intraperitoneal injections of 1 × 10<sup>6</sup> EAC cells were administered to all groups. Group I, designated as the negative control, received intraperitoneal injections of normal saline. Group II was given 25 mg/kg 5-fluorouracil (a conventional drug used in cancer therapeutics).

Groups III, IV, and V received PzMH fraction at doses of 100, 200, and 300 mg/kg body weight, respectively. These doses were administered to the animals on alternate days over a 12-day period following the tumor inoculation (Sur & Ganguly, 1994).

#### 2.4. Calculation of cell growth inhibition

The evaluation of *in vivo* cell growth inhibition was carried out using a methodology outlined by Rahman et al. (2021), with slight modifications (Rahman et al., 2021). On the 12th day of tumor inoculation the mice were sacrificed and cells were collected from the intraperitoneal cavity. Volume of each tumor was recorded and then cells were rinsed with 0.9% normal saline twice. The viability of cells was determined using trypan blue to identify the viable cells, and the cells were counted using haemocytometer. Viable cells were used for further experiments. The formula presented below was used to compute the percentage of cell growth inhibition:

$$\% \text{ Cell growth inhibition} = (1 - (T_t/T_c)) \times 100$$

$T_t$  is average number of tumor cells in treatment groups

$T_c$  is average number of tumor cells in control group

#### 2.5. Cell cycle analysis using flowcytometry

The BD cycle DNA kit was used to examine the cell cycle phase distribution. The isolated cells were fixed in 1 ml of 70% cold ethanol, stored at  $-20^\circ\text{C}$  for 2 h, and rinsed with PBS following incubation. Then 50  $\mu\text{l}$  of trypsin buffer solution was added and incubated for 5 min at  $37^\circ\text{C}$ . After that 50  $\mu\text{l}$  trypsin inhibitor and RNase buffer solution was added and kept for 10 min then 50  $\mu\text{l}$  of cold PI stain solution was added and kept on ice for 30 min and distribution of cell cycle phases examined using flow cytometer (BD accuri C6) (Islam et al., 2015).

#### 2.6. Measurement of apoptosis using Annexin/FITC V double staining

Cells collected from both the control and treated groups were thoroughly rinsed with PBS and then suspended again in a binding buffer (100  $\mu\text{l}$ ). Subsequently, they were subjected to Annexin V-FITC conjugate and propidium iodide treatment, with each reagent applied in a 5  $\mu\text{l}$  volume, for a period of 10 min in a dark at room temperature. Then the percentage of live, early apoptotic (EA), late apoptotic (LA) and necrotic cells in treatment and control groups was verified using BD accuri C6 flow cytometer.

#### 2.7. Evaluation of morphological changes in cells for the detection of apoptosis

The nuclear morphology of control and treatment group cells was studied by staining the cells with DAPI dye. The formation of apoptotic bodies and cell death was studied by staining the cells with acridine orange/ethidium bromide (5  $\mu\text{g}/\text{ml}$ ). The isolated cells were incubated in acridine orange/ethidium bromide (AO/EtBr) (5  $\mu\text{g}/\text{ml}$ ) and DAPI (10  $\mu\text{g}/\text{ml}$ ) separately for 15 min in the dark and were seen under a fluorescent microscope and images were captured.

#### 2.8. Western blotting to measure apoptosis

The protein was extracted from the isolated cells by lysing them using the RIPA lysis buffer. Briefly, cells were incubated in RIPA lysis buffer for a period of 30 min at  $4^\circ\text{C}$  with occasional stirring. The cells were centrifuged at  $4^\circ\text{C}$  for 20 min at 13,500 rpm (revo-

lutions per min). Supernatant containing protein was collected and quantified using Bradford's method of protein estimation. The PVDF membrane was used to transfer the 30  $\mu\text{g}$  protein per sample resolved on 10 % SDS-PAGE gel. Membrane was incubated in 5% skimmed milk for 2 h to block the non-specific sites followed by overnight incubation with primary antibodies (cleaved-caspase 3, cleaved-caspase 9, Bcl-2,  $\beta$ -actin) at  $4^\circ\text{C}$ . Afterwards, membrane was incubated with secondary antibody at room temperature for 2 h. Then membrane was rinsed with TBST buffer twice and bands were developed using ECL reagent and quantified using Image J software.

#### 2.9. Repeated-dose sub-acute toxicity study

This experiment was used to evaluate the impact of the PzMH fraction on animals in a 28-day repeated dosing trial according to the guidelines set forth by OECD 407 (2008b) (Thakur et al., 2022). The animals were distributed into four sets, each comprising five animals. Group I, serving as the control, was administered 0.5 ml of saline intraperitoneally (i.p.). Meanwhile, groups II, III, and IV, designated as the experimental groups, received the PzMH fraction at varying doses: low (150 mg/kg), medium (300 mg/kg), and high (600 mg/kg). Following the 28-day dosing period, blood samples (0.5 ml) were obtained for haematological examination (using Medonic M32 Hematolyzer) and biochemical (using Avantor Benesphera C71 Clinical Biochemical Analyzer) parameters. Additionally, animals were sacrificed for histopathological examination. The brain, kidney, heart, lungs, and liver were excised, and any excess fat was carefully removed. Subsequently, these tissues were immersed in 10% formalin for fixation. Following fixation, the samples were embedded in paraffin blocks and sliced into sections and H&E (haematoxylin & eosin) staining was performed for histopathological analysis (Thakur et al., 2022).

#### 2.10. PzMH fraction phytoconstituents by GC-MS analysis

The Shimadzu GCMS-TQ8050 NX system was used for the GC-MS analysis. GC-MS detection was done using 70-eV electron ionization device. Helium was used as a carrier gas (99.999 %) with an injection volume of 1  $\mu\text{l}$  and a continuous flow rate (1 ml/min). The oven temperature was  $70^\circ\text{C}$ , with  $200^\circ\text{C}$  ion-source temperature. The GC took 63 min to complete.

#### 2.11. Statistical analysis

The one-way analysis of variance (ANOVA) was used to calculate significant differences between the means, with SPSS software utilized for this analysis. Significance was determined at the  $p \leq 0.05$  level. All findings are presented as Mean  $\pm$  Standard Error (SE).

### 3. Results

#### 3.1. Acute toxicity

The results of the acute toxicity study of PzMH fraction administered at 300 and 2000 mg/kg b.w. doses are presented in the Table 1. No clinical signs of toxicity, such as convulsions, tremors, diarrhoea, salivation, coma or lethargy, were observed in animals treated with 300 mg/kg b.w., and no mortality was observed in either the first or confirmatory steps. However, administration of PzMH fraction at a dose of 2000 mg/kg b.w. resulted in 100% mortality in the first and confirmatory steps. Therefore, from the above results, PzMH fraction was found to be in GSH category 4 according

**Table 1**  
Summary of Acute toxicity study.

Steps	Test Item	Dose (mg/kg b.w.)	No. of animals	Clinical Signs*	Mortality
Step-I	PzMH	300	3	–	0/3
Step-I Confirmation	PzMH	300	3	–	0/3
Step-I	PzMH	2000	3	Mild	3/3
Step-I Confirmation	PzMH	2000	3	Mild	3/3

to Annexure 2c, and the LD<sub>50</sub> cut-off value was determined to be 500 mg/kg b.w.

**3.2. PzMH fraction inhibits cell proliferation of EAC cells in vitro**

EAC cells showed that PzMH fraction possesses growth inhibitory activity on cancer cells as evidenced by MTT assay. It was found to cause 50% cell death at 42.74 µg/ml concentration. PzMH fraction caused 89% inhibition of cell proliferation at the highest tested concentration (500 µg/ml) as compared to standard drug 5-fluoro uracil which caused 93.63% inhibition at 500 µg/ml concentration (Table 2).

**3.3. Cell growth inhibition in-vivo**

Since the PzMH fraction exhibited excellent growth inhibitory activity against EAC cells *in-vitro*, we investigated its cancer growth inhibitory activity in *in-vivo* model. PzMH fraction was found to inhibit 32.86, 60.48 and 79.05% cell growth at 100, 200 and 300 mg/kg doses respectively. 5-Fluorouracil (The standard drug) inhibited 84.28% cells at 25 mg/kg concentration (Fig. 1., Table 3.).

**Table 2**  
Cytotoxic potential of PzMH fraction against EAC cells *in vitro*.

Concentration (µg/ml)	% Growth Inhibition ( <i>in-vitro</i> )	
	PzMH fraction	5-Fluoro Uracil
15.625	28.67 ± 1.58 <sup>a</sup>	23.80 ± 5.38 <sup>a</sup>
31.25	47.40 ± 4.43 <sup>b</sup>	44.50 ± 2.86 <sup>b</sup>
62.5	59.63 ± 1.52 <sup>c</sup>	63.70 ± 1.82 <sup>c</sup>
125	67.57 ± 1.98 <sup>c</sup>	75.65 ± 1.01 <sup>cd</sup>
250	82.00 ± 0.78 <sup>d</sup>	82.16 ± 0.71 <sup>de</sup>
500	89.04 ± 1.05 <sup>d</sup>	93.63 ± 1.25 <sup>e</sup>
GI <sub>50</sub> (µg/ml)	<b>42.74</b>	<b>43.38</b>
R <sup>2</sup>	<b>0.981</b>	<b>0.9613</b>
Regression equation	<b>y = 17.048ln(x) – 14.017</b>	<b>y = 19.542ln(x) – 23.673</b>

**3.4. Effect of PzMH fraction on cell cycle phase distribution**

BD Accuri C6 flow cytometer was used to study the effect of PzMH fraction on different stages of cell cycle. Nearly 50 % of the cells isolated from the control group of EAC bearing mice were in the S phase of cell cycle, 25 % cells were in M phase and 17% cells were in the G<sub>0</sub>/G<sub>1</sub> stage. The cells isolated from the treatment group (100 mg/kg body weight) showed, 71% cells in G<sub>0</sub>/G<sub>1</sub>, 17.22 % in S and 6.25 % in the M stage of the cell cycle (Fig. 2 A.).

**3.5. Detection of apoptosis in PzMH treated mice**

Apoptosis inducing potential of PzMH fraction was evaluated through Annexin-V/FITC double staining using BD C6 flow cytometer. The cells isolated from the treated mice showed nearly 36% live cells, 30% early apoptotic (EA), 33% late apoptotic (LA) and 0.7% necrotic cells. Whereas, untreated control group showed 62% live cells, 17% early apoptotic, 20% late apoptotic and 0.5 % necrotic cells (Fig. 2C.).

**3.6. Assessment of the nuclear morphology of cells using confocal microscopy**

Apoptosis is a form of regulated cell death that hinders the proliferation of cells (Jan and Chaudhry 2019). According to Gallardo-Escarat et al. (2007), the fluorescent nuclear dye DAPI staining has a strong affinity for DNA (GALLARDO-ESCÁRATE et al., 2007). DAPI nuclear staining showed condensation and fragmentation of chromatin in PzMH treated cells. Fig. 3A depicts the untreated EAC cells undamaged nucleus, whereas PzMH fraction treated mice showed increased apoptosis. Using DAPI staining to examine the impact of PzMH fraction on EAC cells revealed the occurrence of nuclear changes that signify apoptosis (Fig. 3A).

**3.7. Evidence of apoptosis by AO/EtBr dual staining**

The PzMH fraction treated EAC cells stained with AO/EtBr showed rise in apoptosis as opposed to the control cells. In contrast to EAC cells treated with PzMH fraction, which showed a bright



**Fig. 1.** Morphological changes in the tumor size in PzMH fraction treated mice as compared to control and standard drug.

**Table 3**  
In vivo EAC cell growth inhibition possessed by PzMH fraction.

Experiment name	Drug name	Dose mg/kg b.w.	Mean of EAC cells 12 days after tumor inoculation	% Growth Inhibition
EAC Bearing mice	Control	–	$7 \times 10^7 \pm 0.66$	–
5 -fluorouracil	Standard Drug	25	$1.1 \times 10^7 \pm 0.42$	84.28
PzMH	Experimental drug	100	$4.7 \times 10^7 \pm 0.47$	32.86
		200	$2.78 \times 10^7 \pm 0.30$	60.48
		300	$1.47 \times 10^7 \pm 0.45$	79.05

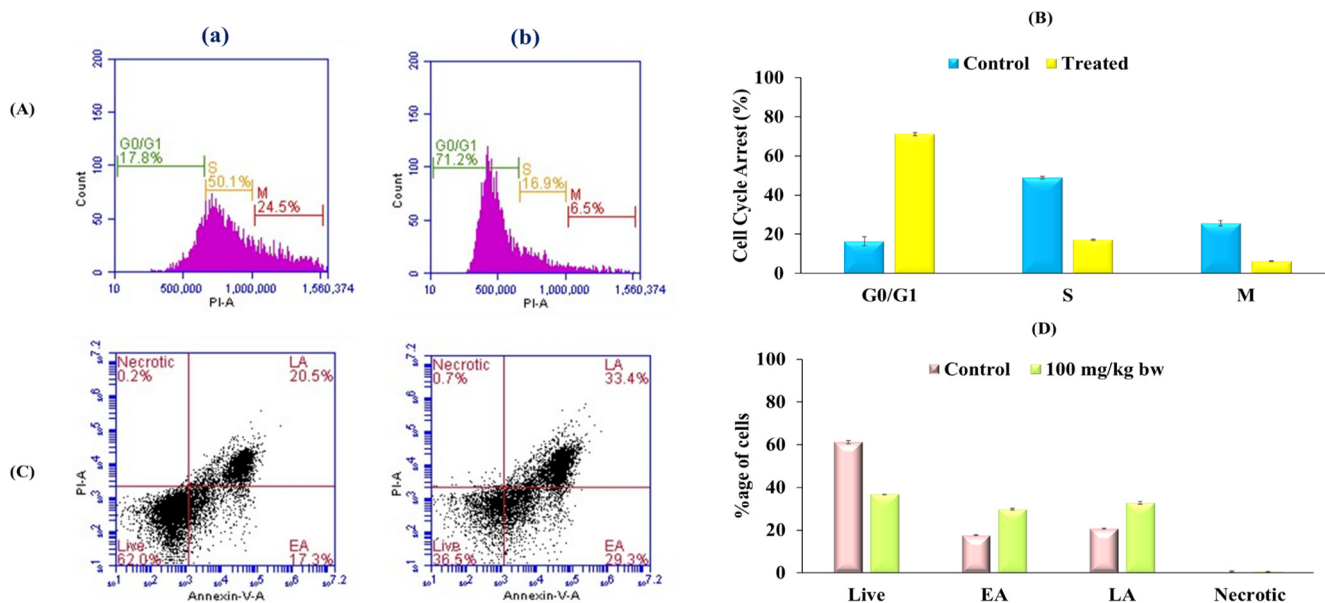


**Fig. 2.** (A) PzMH fraction caused cell cycle arrest at G<sub>0</sub>/G<sub>1</sub> Stage of Cell cycle. (B) Bar graph represents percentage of control and PzMH treated cell at different cell cycle stages. (C) Phase distribution analysis using flow cytometer. Lower left quadrant represents live cells, lower right quadrant represents cells in early apoptosis (EA), upper right quadrant represents cells in late apoptosis (LA) and upper left quadrant represents necrotic cells. (D) Bar graph represents percentage of cells in different stages of apoptosis. (a) Control Cell (b) Cells treated with PzMH fraction (100 mg/kg body weight).

green nucleus as an indication of early apoptosis, viable cells (control EAC cells) displayed green staining (Fig. 3B). AO/EtBr double staining showed the signs of apoptosis and DNA damage. Live cells are stained green, apoptotic and dead cells are stained with yellowish-orange and red colour respectively.

### 3.8. Western blotting

Western blotting was performed to understand the underlying mechanism for the anticancer activity of PzMH fraction. Expressions of cleaved-caspase 3, cleaved-caspase 9 and Bcl-2 proteins were quantified and increase in the expression of cleaved-caspase 3 and cleaved-caspase 9 was observed whereas the expression of anti-apoptotic protein Bcl-2 was decreased in the PzMH treated mice (Fig. 4).

## 4. Sub-acute toxicity studies

### 4.1. Body weight and feed intake

The present study assessed the potential toxicity of PzMH fraction following a 28-day intraperitoneal administration in rats. Body weight changes were evaluated in the treated rats as compared to the control group, and it was observed that there were no significant changes observed in the PzMH fraction treated groups. Specifically, the female rats in Groups I, II, III, and IV showed a percentage gain in body weight of 23.9%, 23.2%, 14.2%, and 21.7%, respectively, over the course of the 28-day treatment

period. Moreover, there were no notable alterations in the feed intake of the treated rats as a result of the treatment when compared to the control group.

### 4.2. Histopathological studies

The histopathological examination conducted using H & E staining demonstrated that the brain sections of control mice exhibited a distinct separation between the molecular layer and granule cell layer. Similarly, the heart sections of these mice displayed myocardial fibers with branching patterns, containing myocyte nuclei. Some areas of the heart slide also exhibited clearly visible blood vessels. Moreover, the kidney sections of the control mice revealed the presence of Bowman’s capsule and glomerulus. The control mice’s liver and lungs section showed normal hepatocytes and alveoli, respectively. Comparatively, no notable alterations were noticed in the histopathology of the kidney, liver, brain, heart and lungs of the mice treated with PzMH compared to the control group (Fig. 5).

### 4.3. Blood biochemistry

Table 4 presents the biochemical results from the 28-day repeated dose toxicity assessment of the PzMH fraction, comparing it to the control group. After the 28-day treatment period, there were no notable differences in any of the biochemical parameters between the treatment groups and the negative control group.

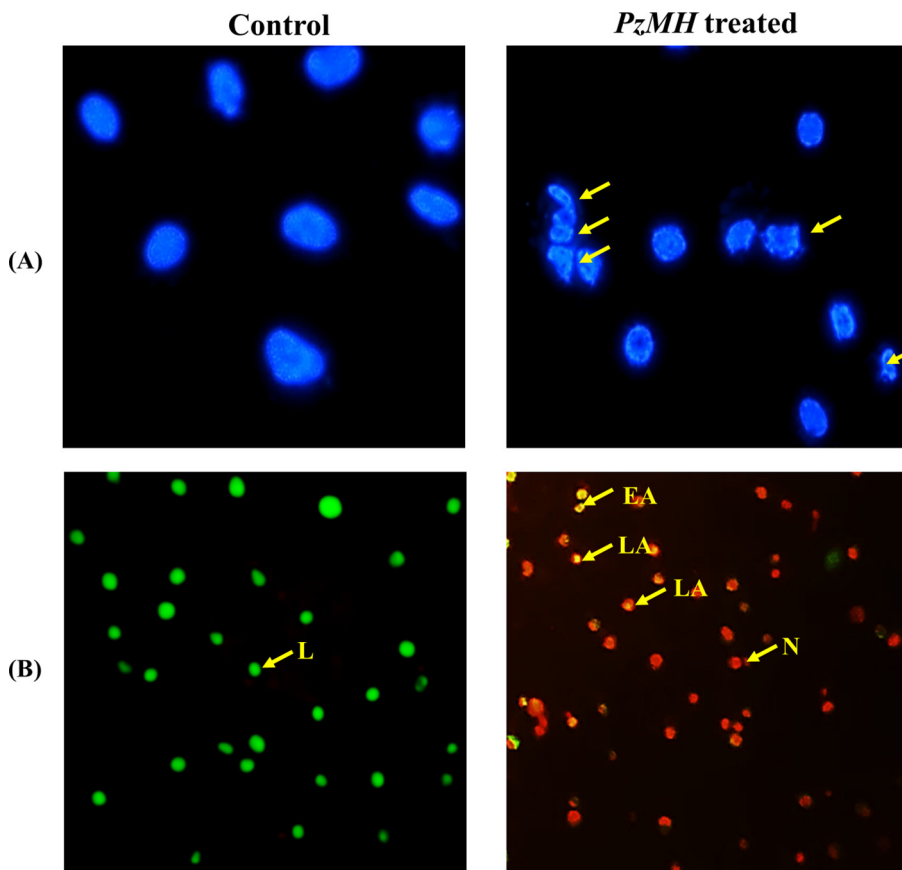


**Fig. 3.** Photomicrographs of EAC cells isolated from control and *PzMH* fraction treated mice. **(A)** EAC cells stained with DAPI. Arrows indicate nuclear fragmentation and shrinkage. **(B)** EAC cells stained with acridine orange/ethidium bromide. Green colour shows live cells, yellowish orange colour shows apoptotic cells and red colour shows dead cells.

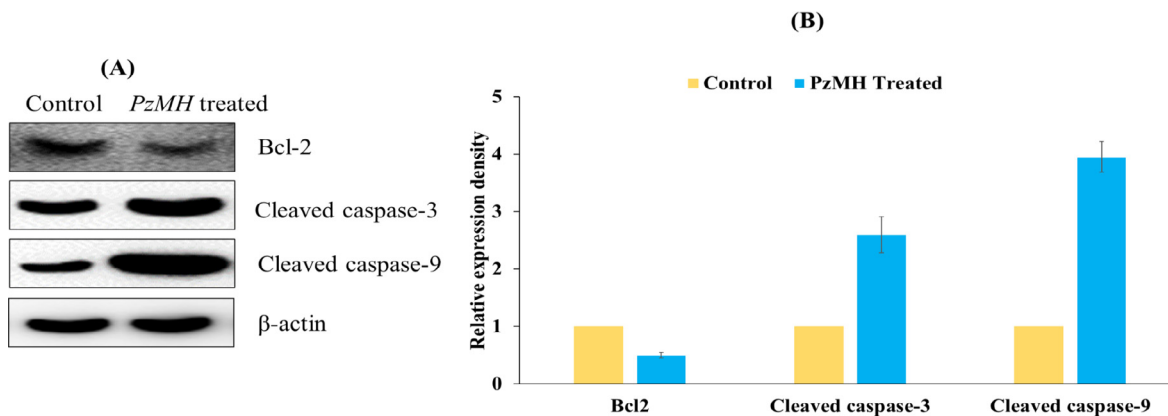


**Fig. 4.** **(A)** An Expression level of Bcl-2, cleaved-caspase3, and cleaved-caspase 9 proteins in EAC cells as detected using Western blotting. **(B)** Bar graph showing densitometric analysis of Bcl-2, caspase-3, and caspase-9 protein bands in Western blotting in *PzMH* treated and control cells. Band density was measured and normalized to that of  $\beta$ -actin.

4.4. Blood hematology

Table 4 displays the hematological results obtained from the 28-day oral toxicity assessment of the *PzMH* fraction, comparing it to the control group. The analysis of blood hematological profiles on the 28th day revealed no significant distinctions between the treatment groups and the control group.

GRA-Granulocytes; HCT-Haematocrit; HGB-Haemoglobin; LYM-Lymphocytes; MCHC-Mean Corpuscular Haemoglobin Concentration; MCH-Mean Corpuscular Haemoglobin; MCV-Mean Corpuscular Volume; MID-Mid-Range Absolute Count; MPV-

Mean Platelet Volume; PCT-Procalcitonin; PLC-Platelet larger cell ratio; PLT-Platelets; RBC- Red Blood Cells; RDW-Red cell distribution; SGOT- Serum Glutamic Oxaloacetic TransaminaseSGPT-Serum Glutamic Pyruvic Transaminase, WBC-White Blood Corpuscles.

4.5. GC-MS analysis

*PzMH* fraction showed the presence of *trans*-cinnamic, lawsone, 4-hydroxy benzaldehyde and plumbagin as major compounds in GC-MS analysis (Fig. 6.).

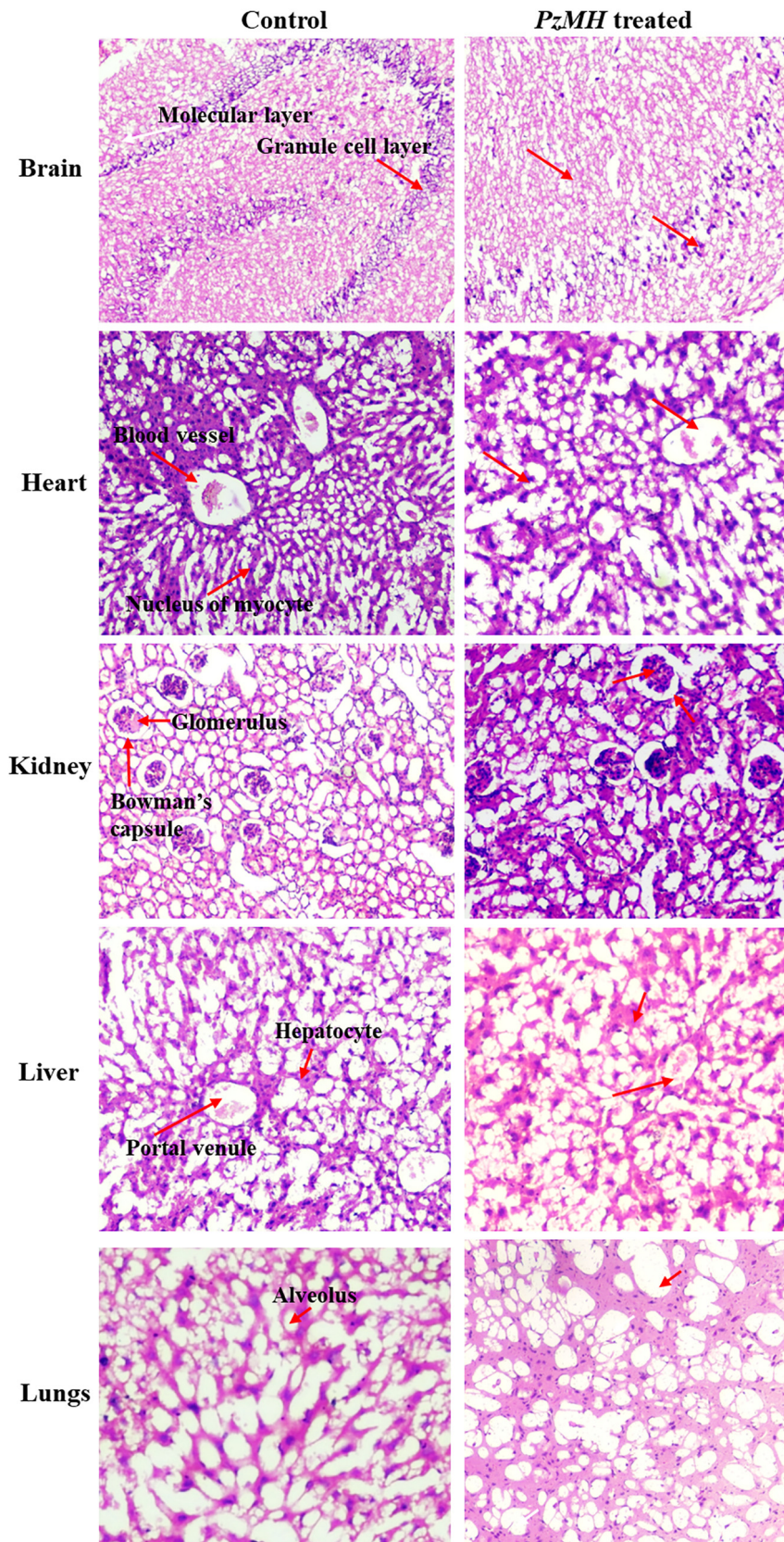
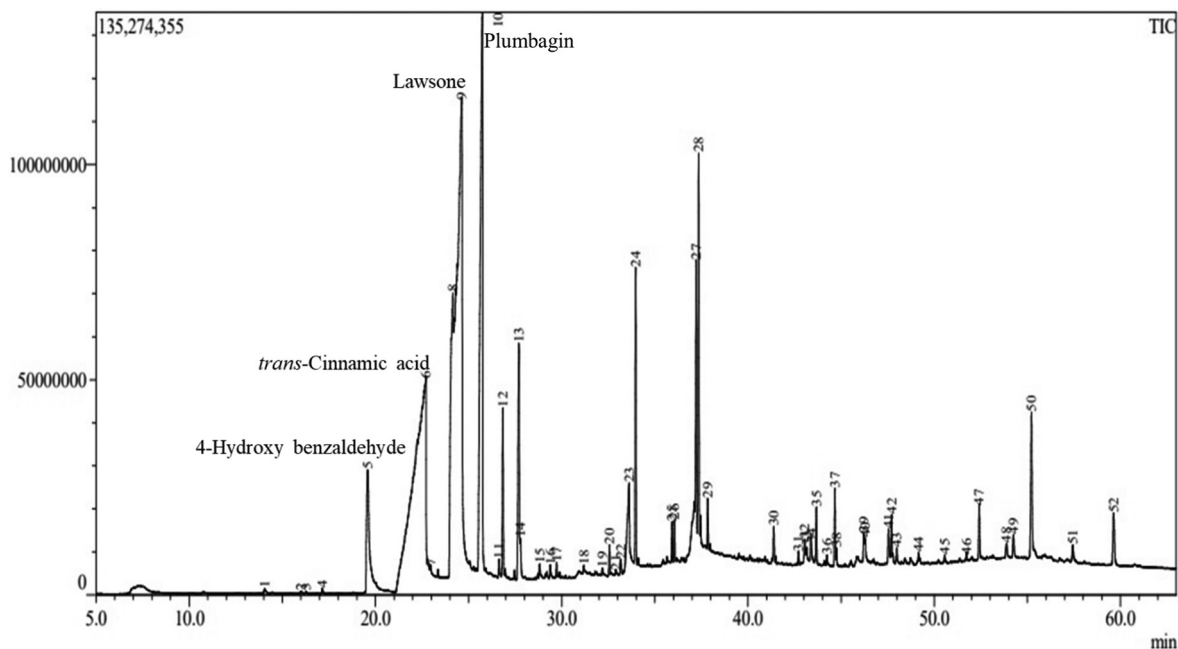


Fig. 5. Photomicrographs of different organs showing histopathology of control and *PzMH* treated mice.

**Table 4**  
Summary of haematological and biochemical parameters in in sub-acute toxicity studies comparing the control group to the groups treated with PzMH fraction after 28 days.

Haematological Parameters	Control	PzMH Fraction (mg/kg b.w.)	
		300	600
WBC	2.10 ± 0.11 <sup>a</sup>	1.40 ± 0.26 <sup>ab</sup>	0.88 ± 0.05 <sup>b</sup>
LYM (%)	1.27 ± 0.18 <sup>a</sup>	0.90 ± 0.15 <sup>a</sup>	0.68 ± 0.06 <sup>a</sup>
MID (%)	0.16 ± 0.03 <sup>a</sup>	0.11 ± 0.05 <sup>a</sup>	0.05 ± 0.01 <sup>a</sup>
GRA (%)	0.34 ± 0.08 <sup>a</sup>	0.27 ± 0.03 <sup>a</sup>	0.25 ± 0.01 <sup>a</sup>
HGB (%)	9.97 ± 0.74 <sup>a</sup>	5.07 ± 0.99 <sup>b</sup>	3.57 ± 0.29 <sup>b</sup>
MCH (%)	19.37 ± 0.40 <sup>a</sup>	20.8 ± 2.32 <sup>a</sup>	17.60 ± 0.65 <sup>a</sup>
MCHC (%)	30.93 ± 2.34 <sup>a</sup>	40.00 ± 5.39 <sup>a</sup>	28.57 ± 0.66 <sup>a</sup>
RBC	4.62 ± 0.54 <sup>a</sup>	3.90 ± 0.33 <sup>a</sup>	3.32 ± 0.10 <sup>a</sup>
MCV	54.93 ± 1.44 <sup>a</sup>	53.53 ± 1.42 <sup>a</sup>	61.07 ± 1.10 <sup>b</sup>
HCT	29.97 ± 1.79 <sup>a</sup>	27.63 ± 0.43 <sup>a</sup>	26.37 ± 0.78 <sup>a</sup>
RDW (%)	19.43 ± 0.87 <sup>a</sup>	13.33 ± 1.45 <sup>b</sup>	18.47 ± 0.64 <sup>a</sup>
PLT	732.67 ± 30.91 <sup>a</sup>	547.67 ± 16.33 <sup>b</sup>	298.00 ± 30.07 <sup>c</sup>
MPV	6.63 ± 0.59 <sup>a</sup>	8.43 ± 0.73 <sup>a</sup>	8.97 ± 0.23 <sup>a</sup>
PDW (%)	39.87 ± 2.01 <sup>a</sup>	47.03 ± 1.01 <sup>b</sup>	49.87 ± 0.66 <sup>b</sup>
PCT	0.58 ± 0.03 <sup>a</sup>	0.46 ± 0.09 <sup>a</sup>	0.41 ± 0.04 <sup>a</sup>
P-LC (%)	13.63 ± 1.45 <sup>a</sup>	17.67 ± 0.75 <sup>a</sup>	19.20 ± 1.15 <sup>a</sup>
Biochemical Parameters	Control	PzMH Fraction (mg/kg b.w.)	
		300	600
Alkaline phosphatase (IU/L)	63.97 ± 3.50 <sup>a</sup>	58.83 ± 1.83 <sup>a</sup>	56.07 ± 3.26 <sup>a</sup>
Urea (g/l)	00.50 ± 0.05 <sup>a</sup>	00.39 ± 0.03 <sup>a</sup>	00.35 ± 0.03 <sup>a</sup>
Creatinine (mg/dl)	00.54 ± 0.03 <sup>a</sup>	00.46 ± 0.03 <sup>a</sup>	00.44 ± 0.02 <sup>a</sup>
SGPT (IU/L)	113.9 ± 3.44 <sup>a</sup>	110.5 ± 2.11 <sup>a</sup>	108.1 ± 1.84 <sup>a</sup>
SGOT (IU/L)	75.00 ± 0.99 <sup>a</sup>	73.47 ± 1.33 <sup>a</sup>	71.40 ± 1.38 <sup>a</sup>
Total bilirubin (mg/dl)	00.75 ± 0.02 <sup>a</sup>	00.71 ± 0.04 <sup>a</sup>	00.67 ± 0.02 <sup>a</sup>
Glucose (mg/dl)	147.6 ± 3.06 <sup>a</sup>	144.7 ± 3.27 <sup>a</sup>	138.83 ± 1.93 <sup>a</sup>



**Fig. 6.** GCMS Chromatogram of PzMH fraction.

### 5. Discussion

The work presented in this study evaluated the anticancer potential of PzMH fraction isolated from *Plumbago zeylanica* L. roots. In this study the cytotoxic potential of PzMH fraction against EAC cells was quantified using MTT assay. The results showed concentration-dependent growth inhibition of EAC cell and 50% cell death was marked at 42.74 µg/ml concentration of PzMH fraction which is comparable to standard drug 5-fluoro uracil which showed 50% cell death at 43.38 µg/ml concentration. Miah *et al.*,

(2020) reported that *Abroma augusta* methanolic bark extract induced toxicity in EAC cells (Miah *et al.*, 2020). The *in vivo* anti-cancer potential of PzMH fraction was carried out on mice model bearing EAC cells and the results were compared with standard drug 5-fluorouracil. 79.05 % growth reduction was calculated at 300 mg/kg body weight (i.p.) dose of PzMH fraction whereas 84.28% growth reduction was shown by 5-fluorouracil at 25 mg/kg body weight (i.p.) dose. The literature survey has reported that 5-fluorouracil (5-FU) exhibits strong protective activity against malignancies in various rodent models. 5-FU is a widely used

chemotherapeutic drug for cancer treatment in several countries (Yosefi et al., 2022) and is considered an alternative medicine. It is employed as a chemotherapeutic agent to combat cancer and other health-related risks (Grem, 2000). Consequently, 5-FU has been established as a standard drug for positive control in numerous cancer models (Adam et al., 2022; Miura et al., 2010; Zhang et al., 2008), making it a suitable choice for our present study.

Kumar et al., 2015 reported that hydroalcoholic extract of *Plumbago Zeylanica* at different doses of 27.5, 55, and 110 mg/kg body weight in rodent model. In acute lethality study of hydroalcoholic extract of *P. zeylanica* was given orally to the animals at dosages of extract of *P. zeylanica* was 928.4 mg/kg (550–1750 mg/kg) showed no toxicity and mortality (Kumar et al., 2015).

The cell division is securely regulated through various conserved mechanisms to produce two genetically identical cells. Acting as surveillance systems, cell cycle checkpoints play a crucial role in preventing the accumulation and dissemination of genetic errors during cellular division. *PzMH* fraction arrested the cell cycle progression at  $G_0/G_1$  stage of the cell cycle. In the *PzMH* treated group, 71% of cells were observed in the  $G_0/G_1$  stage of the cell cycle, while the control group had only 17% of cells in the  $G_0/G_1$  stage. Furthermore, an examination of the S phase distribution revealed that the *PzMH* treated group exhibited a significantly lower percentage of cells in the S phase (17.22%) compared to the control group (25%). Kar et al. (2022) reported that methanolic leaf extract of *Mimusops elengi* arrested EAC cells in  $G_0/G_1$  stage of cell cycle (Kar et al., 2022).

Apoptosis plays a vital role in preserving cellular balance in healthy tissues, malfunctioning in this mechanism enables cancer cells to evade standard therapy, leading to treatment resistance (Singh & Lim, 2022). *PzMH* fraction was observed to be very effective in eliciting apoptosis in EAC cells, as evidenced by microscopic examination and flow cytometric analyses. The Annexin V/FITC double staining technique, using flow cytometer, revealed a significant increase in early apoptotic cells (30%) and late apoptotic cells (33%) within the *PzMH* treated group, in contrast to the control group, where early apoptotic cells constituted 17%, and late apoptotic cells comprised 20%. DAPI nuclear staining and AO/EtBr double staining techniques were utilized to assess apoptosis-related changes, revealing characteristic indications of apoptosis, including apoptotic bodies, DNA damage, and chromatin condensation.

Caspase protease family members are essential in orchestrating the initiation and execution of apoptosis. Upon activation, they engage in cleaving various structural and regulatory proteins, leading to the internal dismantling of the cell. These proteolytic events are responsible for the typical manifestations of apoptosis, encompassing nuclear condensation, DNA fragmentation, and plasma membrane blebbing (Qian et al., 2022). *PzMH* fraction upregulated the expression of caspases, while concurrently downregulating the expression of the Bcl2 protein as compared to the control group. Methanolic extract of *Arthrocnemum machrostachyum* was found to upregulate caspase-3 and downregulation of the Bcl2 protein in EAC cells (Sharawi, 2020).

The toxicity studies of the *PzMH* fraction conducted on Swiss albino mice demonstrated no notable alterations in haematological and biochemical parameters. Additionally, the body weight, feed intake, and behavioural patterns of the *PzMH*-treated animals remained unchanged in comparison to the control group. Histological examinations of the organs from the *PzMH*-treated mice revealed no significant differences as compared to the control group. These findings collectively show that *PzMH* does not induce any apparent toxic effects on the tested parameters and organs in Swiss albino mice. Hydroethanolic extracts of *Paullinia pinnata* and *Securidaca longipedunculata* exhibited significant efficacy in reducing the tumor volume of EAC in mice models and demonstrated a favourable safety profile by not inducing any toxicity in normal

mice at the doses that were proven effective in reducing the EAC tumor volume in EAC-bearing mice (Kola et al., 2023).

The remarkable anticancer potential displayed by the *PzMH* fraction can be attributed to the presence of bioactive compounds identified through GC–MS analysis. These compounds include 4-hydroxy benzaldehyde, *trans*-cinnamic acid, lawsone and plumbagin. Notably, 4-hydroxybenzaldehyde, *trans*-cinnamic acid, and lawsone are recognized as potent phytoconstituents with significant therapeutic potential. Previous research has shed light on their anticancer properties, attributed to their remarkable ability to scavenge free radicals, mitigate inflammation and induce apoptosis. (Eun-Ju et al., 2008) investigated the pharmacological potential of 4-hydroxybenzaldehyde. It showed anti-nociceptive, anti-angiogenic and anti-inflammatory activity by suppressing nitric oxide production and reducing ROS levels in lipopolysaccharide-activated RAW264.7 macrophages. Moreover, 4-hydroxybenzaldehyde attenuated the expression of iNOS and/or COX-2, thus conceivably augmenting its pharmacological effectiveness. Li et al. (2017) reported that lawsone inhibited the proliferation of ovarian cancer cells at  $G_0/G_1$  stage by arresting the cell cycle and induced apoptosis by elevating the levels of caspase-3 and Bax proteins while downregulating the expression of Bcl2 (Li et al., 2017).

## 6. Conclusion

In conclusion, our study thoroughly assessed the anti-cancer potential of the *PzMH* fraction against EAC cells. Through both *in vitro* and *in vivo* experiments, our study found that the *PzMH* fraction effectively inhibited cell death in EAC cells through cell cycle arrest at the  $G_0/G_1$  phase and induced apoptosis through elevated levels of cleaved caspase 3 and 8, and reduced levels of Bcl-2. The *PzMH* fraction demonstrated non-toxicity to normal cells at effective doses, offering potential as a therapeutic agent. Phytochemical analysis revealed the presence of bioactive compounds like *trans*-cinnamic acid, 4-hydroxybenzaldehyde, and lawsone, which could support its anticancer properties. These findings suggest the *PzMH* fraction as a promising candidate for further cancer therapeutics.

## Ethics approval

The Institutional Animal Ethics Committee (IAEC) of GNDU, Amritsar approved the protocol for animal experimentation, following the regulation of CPCSEA (Protocol approval No. 226/CPCSEA/2019/25).

## Consent to participate

All authors have provided their consent to participate in the manuscript publication.

## Consent for publication

All authors have provided their consent for the publication of this manuscript.

## Declaration of funding

This research did not receive any specific grant from funding agencies in the public, commercial, or not-for-profit sectors.

## Declaration of competing interest

The authors declare that they have no known competing financial interests or personal relationships that could have appeared to influence the work reported in this paper.

## Acknowledgement

The Centre of Emerging Life Sciences at GNDU, Amritsar, India, as well as DST-PURSE and DST-FIST were gratefully acknowledged by the authors for their assistance and facilities. The authors would like to extend their sincere appreciation to the Researchers Supporting Project Number (RSP2023R350), King Saud University, Riyadh, Saudi Arabia.

## Author contributions

NS, ST, RK, AK, AA, PK, VR, SKJ and SJK drafted the experimental design and NS performed the experiments. NS, ST, RK, AK, AA, D, VR, SKJ, PK and SJK analyzed the data and helped in writing of this manuscript. VR, AK, SJK and PK revised the language of the manuscript. All authors have read and agreed to the published version of the manuscript.

## Appendix A. Supplementary data

Supplementary data to this article can be found online at <https://doi.org/10.1016/j.jksus.2023.102932>.

## References

- Adam, C., Bray, T.L., Pérez-López, A.M., Tan, E.H., Rubio-Ruiz, B., Baillache, D.J., Houston, D.R., Salji, M.J., Leung, H.Y., Unciti-Broceta, A., 2022. A 5-FU Precursor Designed to Evade Anabolic and Catabolic Drug Pathways and Activated by Pd Chemistry In Vitro and In Vivo. *J. Med. Chem.* 65 (1), 552–561. <https://doi.org/10.1021/acs.jmedchem.1c01733>.
- Alvarez-Ortega, N., Caballero-Gallardo, K., Juan, C., Juan-Garcia, A., Olivero-Verbel, J., 2023. Cytoprotective, Antiproliferative, and Anti-Oxidant Potential of the Hydroethanolic Extract of *Fridericia chica* Leaves on Human Cancer Cell Lines Exposed to  $\alpha$ - and  $\beta$ -Zearalenol. *Toxins* 15 (1), 36.
- Bloch, K., Parihar, V.S., Kellomäki, M., Ghosh, S., 2022. Natural compounds from *Plumbago zeylanica* as complementary and alternative medicine. In: *Handbook of Oxidative Stress in Cancer: Therapeutic Aspects*. Springer Singapore, Singapore, pp. 1–28.
- Eun-Ju, L.I.M., Hyun-Jung, K.A.N.G., Hyun-Joo, J.U.N.G., Kyunghoon, K.I.M., Chang-Jin, L.I.M., Eun-Hee, P.A.R.K., 2008. Anti-inflammatory, anti-angiogenic and antinociceptive activities of 4-hydroxybenzaldehyde. *Biomol. Ther.* 16 (3), 231–236.
- Grem, J.L., 2000. 5-Fluorouracil: Forty-Plus and Still Ticking. A Review of its Preclinical and Clinical Development. *Invest. New Drugs* 18 (4), 299–313. <https://doi.org/10.1023/A:1006416410198>.
- Hanahan, D., 2022. Hallmarks of cancer: new dimensions. *Cancer Discov.* 12 (1), 31–46.
- Hashem, S., Ali, T.A., Akhtar, S., Nisar, S., Sageena, G., Ali, S., Bhat, A.A., 2022. Targeting cancer signaling pathways by natural products: Exploring promising anti-cancer agents. *Biomed. Pharmacother.* 150, 113054.
- Huang, M., Lu, J.J., Ding, J., 2021. Natural products in cancer therapy: Past, present and future. *Natural Products and Bioprospecting* 11, 5–13.
- Islam, F., Khanam, J.A., Khatun, M., Zuberi, N., Khatun, L., Kabir, S.R., Lam, A.K.Y., 2015. A p-Menth-1-ene-4, 7-diol (EC-1) from *Eucalyptus camaldulensis* Dnhh. Triggers Apoptosis and Cell Cycle Changes in Ehrlich Ascites Carcinoma Cells. *Phytother. Res.* 29 (4), 573–581.
- Kar, B., Haldar, P.K., Rath, G., Ghosh, G., 2022. Apoptotic and antiproliferative effects of *Mimusops elengi* leaf extract in Ehrlich ascites carcinoma cells. *Journal of Reports in Pharmaceutical Sciences* 11 (1), 98.
- Kashyap, D., Tuli, H. S., Yerer, M. B., Sharma, A., Sak, K., Srivastava, S., et al. 2021. Natural product-based nanoformulations for cancer therapy: Opportunities and challenges. In *Seminars in cancer biology* (Vol. 69, pp. 5–23). Academic Press.
- Kola, P., Manjula, S.N., Metowogo, K., Madhunapantula, S.V., Eklug-Gadegbeku, K., 2023. Four Togolese plant species exhibiting cytotoxicity and antitumor activities lighting polytherapy approach in cancer treatment. *Heliyon* 9 (3).
- Kumar, D., Patil, P., Roy, S., Kholkute, S., Hegde, H., Nair, V., 2015. Comparative toxicity profiles of *Plumbago zeylanica* L. root petroleum ether, acetone and hydroalcoholic extracts in Wistar rats. *AYU (An International Quarterly Journal of Research in Ayurveda)* 36 (3), 329. <https://doi.org/10.4103/0974-8520.182750>.
- Li, P., Xin, H., Liu, W., 2017. Lawsone inhibits cell growth and improves the efficacy of cisplatin in SKOV-3 ovarian cancer cell lines. *Afr. J. Tradit. Complement. Altern. Med.* 14 (5), 8–17.
- Miah, M., Shimu, A. S., Mahmud, S., Omar, F. B., Khatun, R., Mohanto, S. C., et al. 2020. Methanolic Bark extract of *Abroma augusta* (L.) induces apoptosis in EAC cells through altered expression of apoptosis regulatory genes. Evidence-based complementary and alternative medicine, 2020.
- Miura, K., Kinouchi, M., Ishida, K., Fujibuchi, W., Naitoh, T., Ogawa, H., Ando, T., Yazaki, N., Watanabe, K., Haneda, S., Shibata, C., Sasaki, I., 2010. 5-FU Metabolism in Cancer and Orally-Administerable 5-FU Drugs. *Cancers* 2 (3), 1717–1730. <https://doi.org/10.3390/cancers2031717>.
- Morana, O., Wood, W., Gregory, C.D., 2022. The apoptosis paradox in cancer. *Int. J. Mol. Sci.* 23 (3), 1328.
- Ozaslan, M., Karagoz, I.D., Kilic, I.H., Guldur, M.E., 2011. Ehrlich ascites carcinoma. *Afr. J. Biotechnol.* 10 (13), 2375–2378.
- Qian, S., Wei, Z., Yang, W., Huang, J., Yang, Y., Wang, J., 2022. The role of BCL-2 family proteins in regulating apoptosis and cancer therapy. *Front. Oncol.* 12, 985363.
- Rahman, M.M., Reza, A.A., Khan, M.A., Sujon, K.M., Sharmin, R., Rashid, M., Alam, A. K., 2021. Unfolding the apoptotic mechanism of antioxidant enriched-leaves of *Tabebuia pallida* (Lindl.) Miq. in EAC cells and mouse model. *J. Ethnopharmacol.* 278, 114297.
- Safarzaadeh, E., Shotorbani, S.S., Baradaran, B., 2014. Herbal medicine as inducers of apoptosis in cancer treatment. *Advanced pharmaceutical bulletin* 4 (Suppl 1), 421.
- Sathishkumar, K., Chaturvedi, M., Das, P., Stephen, S., Mathur, P., 2022. Cancer incidence estimates for 2022 & projection for 2025: Result from National Cancer Registry Programme, India. *Indian J. Med. Res.*
- Sharawi, Z.W., 2020. Therapeutic effect of *Arthrocnemum macrostachyum* methanolic extract on Ehrlich solid tumor in mice. *BMC complementary medicine and therapies* 20, 1–10.
- Shukla, B., Saxena, S., Usmani, S., Kushwaha, P., 2021. Phytochemistry and pharmacological studies of *Plumbago zeylanica* L.: a medicinal plant review. *Clin. Phytosci.* 7, 1–11.
- Singh, P., Lim, B., 2022. Targeting apoptosis in cancer. *Curr. Oncol. Rep.* 24 (3), 273–284.
- Sur, P., Ganguly, D.K., 1994. Tea plant root extract (TRE) as an antineoplastic agent. *Planta Med.* 60 (02), 106–109.
- Thakur, S., Kour, R., Kaur, S., Jain, S.K., 2022. Spray-Dried Microspheres of Carboplatin: Technology to Develop Longer-Acting Injectable with Improved Physio-Chemical Stability, Toxicity, and Therapeutics. *AAPS PharmSciTech* 23 (5), 128.
- Toxicity-Up, A. O. 2001. OECD guideline for testing of chemicals. Organisation for Economic Co-Operation and Development: Paris, France.
- Yosefi, S., Pakdel, A., Sameni, H.R., Semnani, V., Bandegi, A.R., 2022. Chrysin-Enhanced Cytotoxicity of 5-Fluorouracil-Based Chemotherapy for Colorectal Cancer in Mice: Investigating its Effects on Cyclooxygenase-2 Expression. *Braz. J. Pharm. Sci.* 58. <https://doi.org/10.1590/s2175-97902020e19381>.
- Zhang, N., Yin, Y., Xu, S.-J., Chen, W.-S., 2008. 5-Fluorouracil: Mechanisms of Resistance and Reversal Strategies. *Molecules* 13 (8), 1551–1569. <https://doi.org/10.3390/molecules13081551>.